J Nanostruct 8(4): 350-358, Autumn 2018

RESEARCH PAPER

Synthesis of Magnetic Iron Oxide Nanoparticles and its Application for Simultaneous Determination of Hydrazine and Hydroxylamine

Mohammad Mazloum-Ardakani *, *Mehdi Maleki, Alireza Khoshroo*

Department of Chemistry, Faculty of Science, Yazd University, Yazd, Iran

ARTICLE INFO

Article History:
Received 02 July 2018
Accepted 13 September 2018
Published 01 October 2018

Keywords:
Electrocatalysis
Hydrazine
Hydroxylamine
Magnetic Nanoparticles
Modified Electrodes

ABSTRACT

This work describes the electrochemical properties of magnetic iron oxide nanoparticles (Fe_2O_3 and Fe_3O_4) as highly sensitive sensors for the simultaneous determination of hydrazine and hydroxylamine using a glassy carbon electrode. The electrochemical behavior of hydrazine and hydroxylamine was investigated using cyclic voltammetry, chronoamperometry and differential pulse voltammetry techniques. The results show that, at the modified electrode surface, the peaks of hydrazine and hydroxylamine oxidation were well resolved. Based on differential pulse voltammetry, the oxidation of hydrazine exhibited the dynamic range between 1.0- 1000.0 µM, and the detection limit (3σ) was 0.65 µM. These features will facilitate the determination of hydrazine and hydroxylamine in samples at a magnetic iron oxide modified electrode.

How to cite this article
Mazloum-Ardakani M, Maleki M, Khoshroo A. Synthesis of Magnetic Iron Oxide Nanoparticles and its Application for Simultaneous Determination of Hydrazine and Hydroxylamine. J Nanostruct, 2018; 8(4): 350-358.
DOI: 10.22052/JNS.2018.04.004

INTRODUCTION

Many materials were found to exhibit improved properties at nanoscales [1]. Nanoparticle research is currently an area of intense scientific research, resulting in applications of nanoparticles to areas including catalysis, self-assembly, and spintronics [2–4]. Current scientific research has been focused on developing materials that exhibit such advantages as easy preparation, high stability, low cost, and easy separation from solutions by an external magnetic field [5, 6]. Among various materials, iron oxide nanoparticles (Fe_2O_3 and Fe_3O_4) have received a lot of attention due to their small band gap (2.2 eV), high stability and low cost [7]. Iron oxide magnetic nanoparticles tend to be either paramagnetic or superparamagnetic, with particles approximately 20 nm being classed as the latter. In most cases, superparamagnetic particles (usually Fe_2O_3 and Fe_3O_4) are of interest for *in vivo* applications, as they do not retain any magnetism after removal of the magnetic field [8].

* *Corresponding Author Email: mazloum@yazd.ac.ir*

Hydrazine and its derivatives are widely used as a raw material in industrial and agricultural applications and as a powerful reducing agent in fuel cells [9, 10]. However, hydrazine is a toxic compound. Notably, hydrazine and its derivatives have been reported to cause adverse health effects [11]. Accordingly, a highly sensitive method is necessary for the measurement of hydrazine concentration and the electro oxidation of hydrazine concentration in environmental and medical samples [12, 13]. In addition, hydrazine is used as a raw material in rocket fuel and direct fuel cells, where hydrazine is oxidized to form nitrogen and water; it is another reason for the importance measurement of hydrazine. Among the various methods for the measurement of hydrazine concentration including chromatography, fluorimetry and spectrophotometry, electrochemical methods are practical and attractive because electrochemical instrumentation is usually compact, relatively

inexpensive, reliable and sensitive [14, 15]. As overpotential of hydrazine electro-oxidation is usually high at conventional electrodes, a variety of modified electrodes has been developed to minimize this drawback and also to enhance electron transfer rate [16–18]. Various metal nanoparticles have been used to develop a highly sensitive electrode for hydrazine detection including silver [19], gold [20], nickel, platinum [21], palladium [16] and ruthenium [22]. Although these metals are very efficient in the anodic oxidation of hydrazine, they are too expensive for practical applications.

Hydroxylamine, a derivative of ammonia, is one of the reducing agents widely used in industry and pharmacy [23]. Hydroxylamine is a well-known mutagen, which induces highly specific mutations with the nucleic acid cytosine. Modest levels of hydroxylamine can be toxic to humans, animals and even plants [24]. Therefore, from the industrial, environmental and health viewpoints, development of a sensitive analytical method for the simultaneous determination of hydrazine and hydroxylamine is very important. However, the oxidation peaks of hydrazine and hydroxylamine obtained at a bare glassy carbon electrode occurred at similar potentials resulting in overlapped responses that make it difficult to distinguish between the two peaks [25].

In this work, we used a magnetic iron oxide nanoparticle modified glassy carbon electrode in the electroanalytical catalysis and simultaneous determination of hydrazine and hydroxylamine. The main objective of this work was to develop a method capable of yielding well-resolved electrochemical responses of hydrazine and hydroxylamine during their simultaneous detection. The experimental results indicate that modified glassy carbon electrode facilitates electron transfer on surface of the electrode due unique electrochemical during their simultaneous detection properties, high repeatability and good stability.

MATERIALS AND METHODS

Apparatus and chemicals

Electrochemical measurements were performed using a potentiostat/galvanostat (SAMA 500, Iran). All electrochemical studies were carried out in a conventional three-electrode cell. A saturated calomel electrode (SCE) was used as reference electrode and a platinum wire as the counter electrode. A glassy carbon electrode modified by magnetic iron oxide nanoparticles was used as the working electrode. A Metrohm 781 pH/ion meter was used for pH measurements. A buffer was prepared from from orthophosphoric acid and its salts in the pH range of 2.0–11.0. All solutions were prepared with twice-distilled water Analytical grade $FeCl_2.4H_2O$ and $FeCl_3.6H_2O$ and all other reagents were acquired from Merck (Darmstadt, Germany).

Synthesis of magnetic iron oxide nanoparticles (Fe_2O_3 and Fe_3O_4)

The coprecipitation technique is the simplest and most efficient chemical pathway to obtain magnetic nanoparticles iron oxides (Fe_2O_3 and Fe_3O_4) [26].

Fe_3O_4 magnetic nanoparticles were prepared by coprecipitation of ferric and ferrous ions using NH_3 [27]. Briefly, 4.24 g of $FeCl_3$ and 1.52 g of $FeCl_2$ were dissolved in about 50 mL of twice-distilled and heating with stirring at 50 – 60 ◦C for 0.5 h, to completely dissolved, then 30 ml of NH_3 25% was added dropwise to the solution with vigorous stirring at 50 – 60 ◦C, for 30 min. A black precipitate formed was separated using a magnet. The precipitate was then washed two times using twice-distilled water. Next, 0.01 M HCL was added until pH 7 was obtained, indicating the neutralisation of anionic charges on the nanoparticles. The precipitate was again separated using a magnet and then dried in air. Fe_3O_4 nanoparticles were obtained at the end of this procedure. Aqueous Fe_3O_4 nanoparticles were then oxidized to obtain Fe_2O_3 nanoparticles [28].

$$Fe_3O_4 + 2H^+ \rightarrow Fe_2O_3 + Fe^{2+} + H_2O$$

In this experiment, Fe_3O_4 nanoparticles were dissolved in 100 ml of 0.01 M HNO_3 before the mixture was heated at 90-100 ◦C with stirring for 60 min to completely oxidize the Fe_3O_4 nanoparticles to Fe_2O_3 nanoparticles [20, 22-24].

Electrode Modification Procedure

In fabricating an electrochemical sensor, a glassy carbon electrode (GCE) was initially polished using slurry of alumina on a polishing cloth and then rinsed with twice-distilled water. The GCE was next activated by cycling the potential between 0.0 and 1.3 V in 0.5 M H_2SO_4 solution until a stable cyclic voltammogram was obtained.

A thin-film modified electrode was next prepared. In our work, 10 mg of Fe_3O_4 nanoparticles was dispersed ultrasonically in a mixture 0.5 mL ethanol and 0.1 ml 5% (v/v) nafion. Then, 3 µL of this suspension was dropped to the GCE and left at ambient temperature to air dry for 10 min.

RESULTS AND DISCUSSION

Characterization of the iron oxide nanoparticles

The response of an electrocatalyst is related to its physical morphology of its surface. Fig. 1 displays the scanning electron micrographs of the synthesized iron oxide nanoparticles. It can be seen that microsphere crystals appeared with good dispersion. The Fe_2O_3 being entangled (Fig. 1A) but Fe_3O_4 are gradually freed from the entanglements favoring their alignment (Fig. 1B).

Cyclic voltammetry was used for further characterization of the iron oxide nanoparticles. Fig. 1C shows the cyclic voltammetric behaviors of different modified electrodes in 1.0 mM $K_4Fe(CN)_6$ and 1.0 mM $K_3Fe(CN)_6$ containing 0.1 M KCl solution. Experimental results showed reproducible, well-defined, anodic and cathodic peaks at 0.18 and 0.82 V, respectively. The peak current (I_{pa}) at the Fe_3O_4 / GCE was 1.4 times higher than that at the Fe_2O_3 / GCE, which was attributable to more electroactive sites of Fe_3O_4 exposing on the modified electrode.

The active surface area of the modified electrode was estimated according to the slope of the I_p versus $v^{1/2}$ plot for a known concentration of $K_4Fe(CN)_6$, based on the Randles–Sevcik equation:

$$I_{peak}=2.69\times10^5 n^{3/2} A D^{1/2} C_{bulk} v^{1/2} \quad (1)$$

where I_{peak} is the anodic peak current, A the surface area of the electrode, n the number of electron transfered, D the diffusion coefficient, C_{bulk} the concentration of $K_4Fe(CN)_6$ and v the scan rate. For 1.0 mmol L^{-1} $K_4Fe(CN)_6$ in 1.0 mol L^{-1} KCl electrolyte from the slope of the I_{peak}–$v^{1/2}$

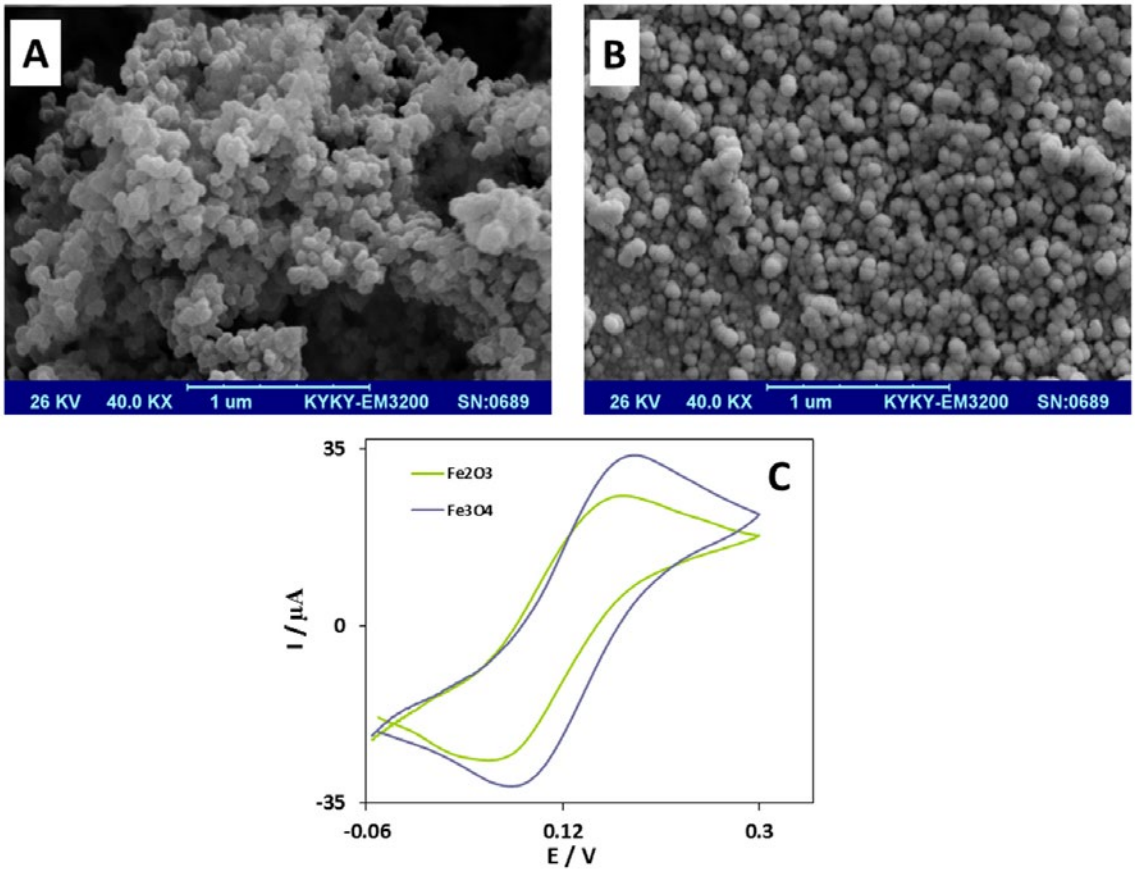

Fig. 1. SEM images of the Fe_2O_3 (A) and Fe_3O_4 (B), (C) CVs of Fe_3O_4 / GCE and Fe_2O_3 / GCE in a 0.1 M KCl solution containing the redox couples of 1.0 mM $K_4Fe(CN)_6$ and 1.0 mM $K_3Fe(CN)_6$.

relation, the microscopic areas were calculated. They were 0.07 and 0.05 cm^2 for Fe_3O_4 / GCE and Fe_2O_3 / GCE, respectively. The results show that the Fe_3O_4 nanoparticle causes the active surface of the electrode to increase.

Electrochemical oxidation of hydrazine at iron oxide nanoparticles / GCE

Cyclic voltammetry of hydrazine at a Fe_3O_4 / GCE and a Fe_2O_3 / GCE in 0.1 M phosphate buffer (pH 8) was conducted. Fig. 2 shows the cyclic voltammetric responses for the electrochemical oxidation of 1.0 mM hydrazine. In curve a, an anodic peak at 0.8 V is related to the oxidation of hydrazine at the bare GCE. As shown in curve b and curve c, when hydrazine was oxidized at a Fe_3O_4 / GCE and a Fe_2O_3 / GCE, a respective peak potential of 0.3 V and 0.4 V was located. These peak potentials are 0.4-0.5 V more negative than that obtained at a bare GCE. Cyclic voltammograms (CVs) exhibited an anodic peak related to the oxidation of hydrazine, but no cathodic peak is found, indicating an irreversible heterogeneous charge transfer in this system. As can be seen Fe_3O_4 has better performance towards oxidation of hydrazine. This effect was attributed to the larger available surface area of the modifying layer due to the nanometer size of the sample [29]. In curve d, there was no observable redox peak in the cyclic voltammogram of 0.1 M PBS at the Fe_3O_4 / GCE, indicating that Fe_3O_4 / GCE itself was not electroactive within the potential window.

The effect of potential scan rate on the cyclic voltammetric oxidation of 0.5 mM hydrazine at the Fe_3O_4 / GCE in 0.1 M phosphate buffer was studied.

Fig. 3A shows a linear plot of the anodic peak current (Ip) from the various cyclic voltammograms in Fig. 3 versus square root of scan rate ($v^{1/2}$) between 5 and 500 mVs^{-1}, indicating that hydrazine oxidation at the Fe_3O_4 / GCE is a diffusion-controlled process. In the determination of the electron transfer coefficient (α) and the number of electron involved in the rate determining (n_α), the results suggest a four-electron (n_α=1) transfer process for the oxidation of hydrazine.

The number of electrons in the overall reaction can be acquired from the slope of the I_p versus plot (n= 4) [26].

$$N_2H_4 \rightarrow N_2 + 4\,H_2O + 4e$$

A Tafel plot from data of the rising part of the current–voltage curve is illustrated in Fig. 3B. The Tafel slope was 105.8 mV $decade^{-1}$ that α equals 0.56.

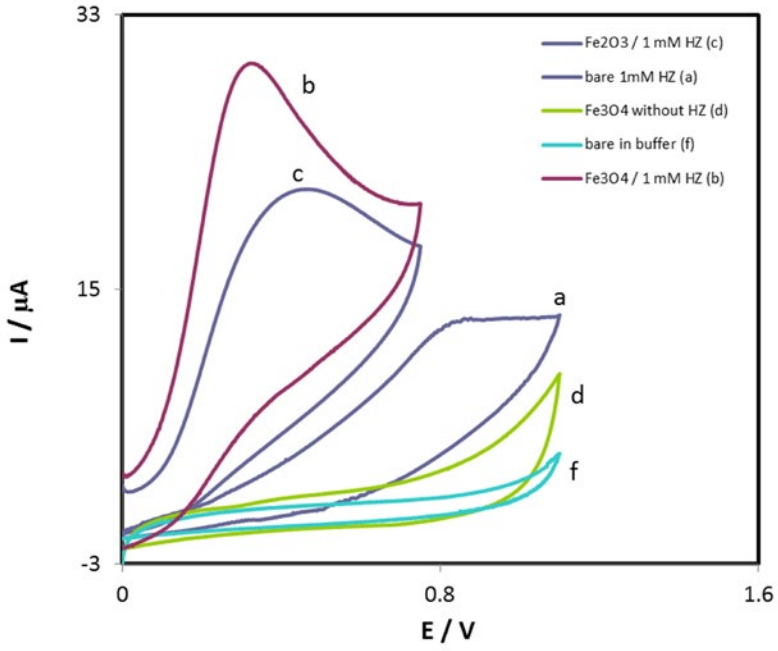

Fig. 2. Cyclic voltammograms for oxidation of 1.0 mM hydrazine in solution of 0.1 mol phosphate buffer at pH=8, (a) bare GCE, (b) Fe_3O_4 / GCE, (c) Fe_2O_3 / GCE, (d) Fe_3O_4 / GCE in phosphate buffer without hydrazine, (f) bare GCE in phosphate buffer without hydrazine. Scan rate: 100 mVs^{-1}.

Chronoamperometric studies for hydrazine

Iron oxide nanoparticles have catalysed the oxidation of hydrazine was also studied by chronoamperometry. Chronoamperograms acquired at different concentrations of hydrazine in aqueous buffered solution (pH 8.0) are presented in Fig. 4. The slopes of the resulting straight lines were then plotted *vs* the hydrazine concentration. The linearity of oxidation current *vs*. $\upsilon^{1/2}$ is shown this current is controlled by diffusion of hydrazine from

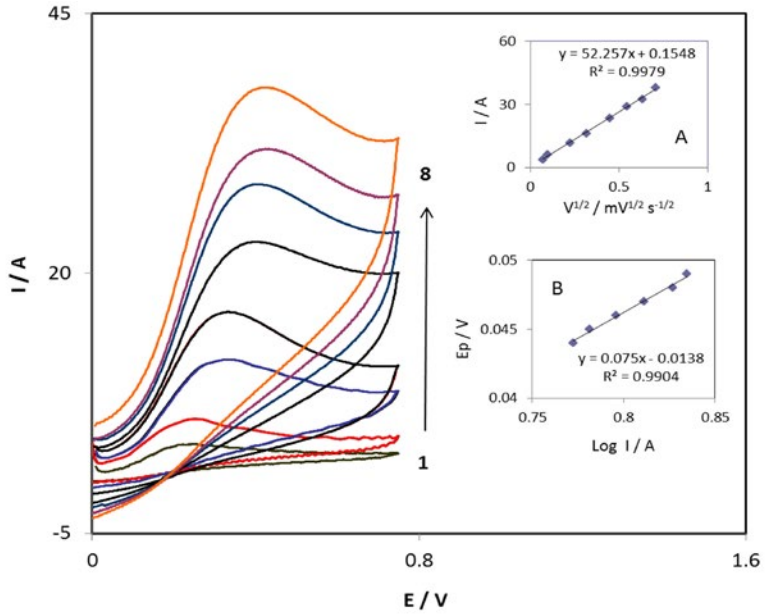

Fig. 3. CVs of 0.5 mM HZ at Fe_3O_4 / GCE in pH 8.0 at various scan rates: numbers 1–8 correspond to 5, 10, 50, 100, 200, 300, 400 and 500 mV s^{-1} scan rates, respectively. Insets: (A) variations of Ip versus the square root ($v^{1/2}$) of scan rate. (B) E_p versus the logarithm current of the scan rate 500 $mVs^{-1/2}$

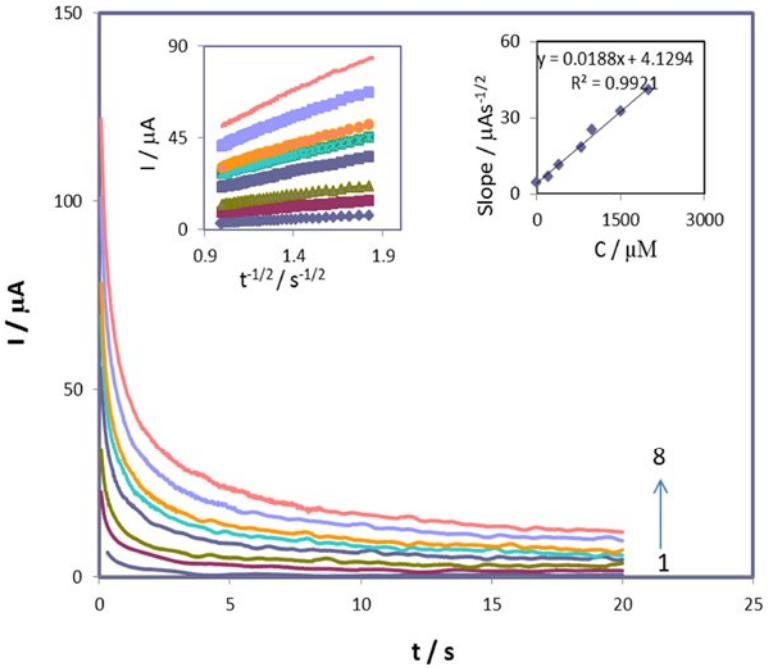

Fig. 4. Chronoamperograms obtained at Fe_3O_4 / GCE in 0.1 M phosphate buffer solution (pH 8.0) for the following concentrations of HZ: 0.0, 200.0, 400.0, 600.0, 800.0, 1000.0, 1500.0 and 2000.0 µM. Insets: (A) plots of I versus $t^{-1/2}$ obtained from chronoamperograms, (B) plot of the slope of the straight lines against the HZ concentration.

bulk solution toward surface of electrode that caused to near-Cottrellian behavior. Therefore, the slope of linear region of Cottrell's plot can be used to estimate the diffusion coefficient (D) of hydrazine. A plot of I versus $t^{-1/2}$ for a Fe_3O_4 / GCE in the presence of hydrazine given a straight line, the slop of such lines can be used to estimate the diffusion coefficient of hydrazine. The mean value of the D found to be 1.84×10^{-4} cm^2 s^{-1}.

Calibration plot and limit of detection for hydrazine

Differential pulse voltammetry (DPV) was used to obtain of detection limit and linear dynamic range of hydrazine. DPV of 1.0-1000.0 µM hydrazine at a Fe_3O_4 / GCE in pH 8.0 phosphate buffer was conducted and the results obtained are shown in Fig. 5. Voltammograms show that the peak currents of hydrazine oxidation at the surface of the Fe_3O_4 / GCE consist of two linear segments with different slopes; a slope of 0.0229 µA µM $^{-1}$ for the first linear segment (1.0–20.0 µM) and a slope of 0.0159 µA μM^{-1} for the second linear segment (20.0–1000.0 µM). The detection limit calculated of hydrazine was obtained 0.65 µM based on signal-to-noise method with considering S/N=3.

Simultaneous determination of hydrazine and hydroxylamine

The ability to determine the electrochemical response of different analytes is one of the important factors for choosing the type of modified electrode. In this work, we use Fe_3O_4 / GCE for the simultaneous determination electrochemical oxidation of hydrazine and hydroxylamine over a range of concentration ratio. The electrochemical behavior of hydrazine and hydroxylamine at a Fe_3O_4 /GCE was studied by cyclic voltammetry. The results obtained are shown in Fig. 6. In Fig. 6A, the cyclic voltammogram of 1.0 mM hydrazine at the Fe_3O_4 /GCE shows an oxidation peak at 0.3 V, compared to 0.8 V in the corresponding voltammogram obtained at the bare GCE. Similary, the cyclic voltammogram of 1.0 mM hydroxylamine at the Fe_3O_4 /GCE (curve b in Fig. 6B) shows an oxidation peak at 0.75 V, compared to 0.95 V in the corresponding voltammogram obtained at the bare GCE (curve a in Fig. 6B). Cyclic voltammorams of a mixture of 1.0 mM hydrazine and 1.0 mM hydroxylamine conducted at a Fe_3O_4 / GCE and a bare GCE are shown in Fig. 5C. In these voltammograms enhancement of the anodic peak

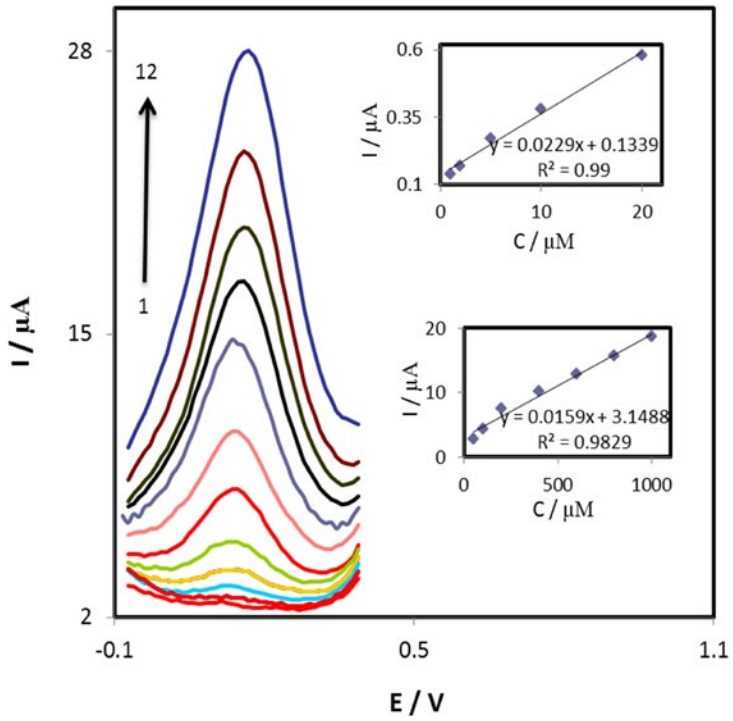

Fig. 5. Differential pulse voltammograms of HZ at Fe_3O_4 / GCE in 0.1 M phosphate buffer solution (pH 8.0), hydrazine concentrations, Inset (1→12): 1.0, 2.0, 5.0, 10.0, 20.0, 50.0, 100.0, 200.0, 400.0, 600.0, 800.0, and 1000.0 µM respectively

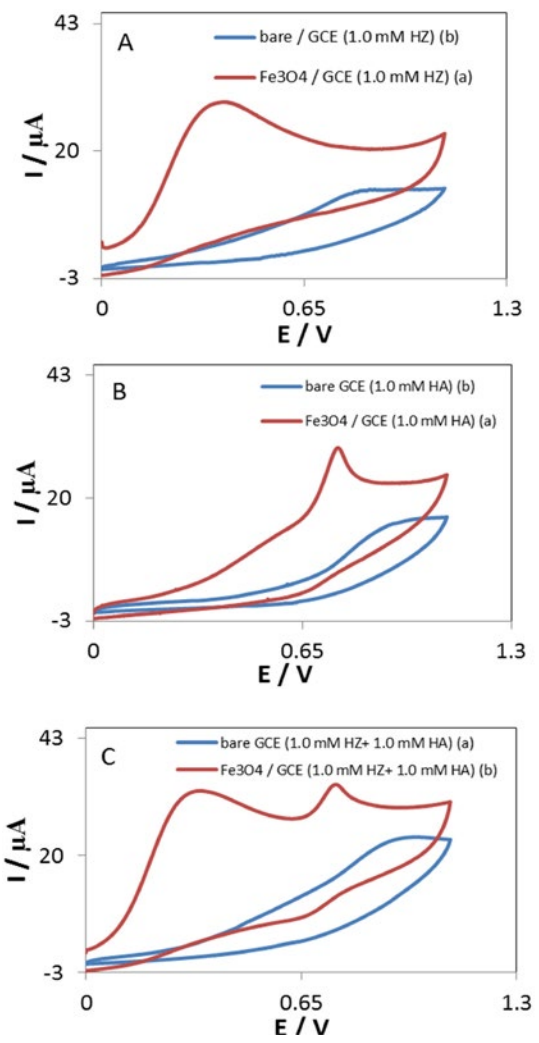

Fig. 6. Comparison of cyclic voltammograms of 1.0 mM HZ (a) and 1.0 mM HA (b) at bare GCE (A) and Fe_3O_4 / GCE (B) and (C) CVs of 1.0 mM HZ + 1.0 mM HA at Fe_3O_4 / GCE (a) and bare GCE (b)

current was observed at the Fe_3O_4 / GCE compared to that at the bare GCE.

Negative shifts in potential with much enhanced peak current indicate an enhanced electron transfer rate for hydrazine and hydroxylamine oxidation at Fe_3O_4 / GCE. According to Fig. 6 C, the CV of bare GCE exhibit only one broad (curve a in Fig. 6 C) without any peak separation for the analytes mixture, while hydrazine and hydroxylamine yielded two well-defined oxidation peaks at the Fe_3O_4 / GCE (curve b in Fig. 6 C). These results show the importance of using Fe_3O_4 / GCE for modifying the electrode surface.

Fig. 7 shows a series of DPVs for simultaneous determination of hydrazine and hydroxylamine at different concentrations using the Fe_3O_4 / GCE. The DPV results show two well distinguished anodic peaks at the surface of Fe_3O_4 / GCE, corresponding to the oxidation of hydrazine and hydroxylamine, respectively (Fig. 7). The peak current increased linearly with increment of hydrazine and hydroxylamine concentration in the range of 50.0 – 500.0 µM and 75 – 750 µM respectively. The sensitivity of the Fe_3O_4 / GCE towards hydrazine in the absence (0.0159 µA μM^{-1}) and presence (0.0156 µA μM^{-1}) of hydroxylamine are virtually the same, which further indicates that the oxidation processes of hydrazine and hydroxylamine at the Fe_3O_4 / GCE electrode are independent and therefore, the simultaneous determination of the two analytes is possible without any interference. Therefore, using the Fe_3O_4 / GCE is a useful, easy and inexpensive way to simultaneously determine hydrazine and hydroxylamine compared with other methods.

The repeatability and stability of Fe_3O_4 / GCE

The durability of Fe_3O_4 / GCE was also assessed through consecutive 100 cyclic voltammetry measurements at a scan rate of 100 mV s^{-1} in solution 1.0 mM hydrazine in phosphate buffer (pH 8.0). In this investigation, the peak potential of hydrazine oxidation atthe modified electrode was unchanged and the current signals showed less than 9.0 % decrease relative to the initial response. The proposed sensor showed a repeatability with a relative standard deviation (RSD) of 2.5% for 15 successive assays.

CONCLUSION

In this work, iron oxide nanoparticle (Fe_2O_3 and Fe_3O_4) modified GCEs were used in the simultaneous oxidation of hydrazine and hydroxylamine. The experimental results indicate that Fe_3O_4 has better performance than Fe_2O_3 towards the oxidation of hydrazine. The modified electrode increase the oxidation currents of hydrazine and hydroxylamine, is shifted to a less positive their oxidation potentials and resolve the overlapping anodic peaks of hydrazine and hydroxylamine into two well-defined peaks and allows their simultaneous determination in solution. High sensitivity and selectivity of the voltammetric responses, and low detection limit, together with the ease of preparation and surface regeneration, make the proposed modified electrode very useful for accurate simultaneous determination of hydrazine and hydroxylamine.

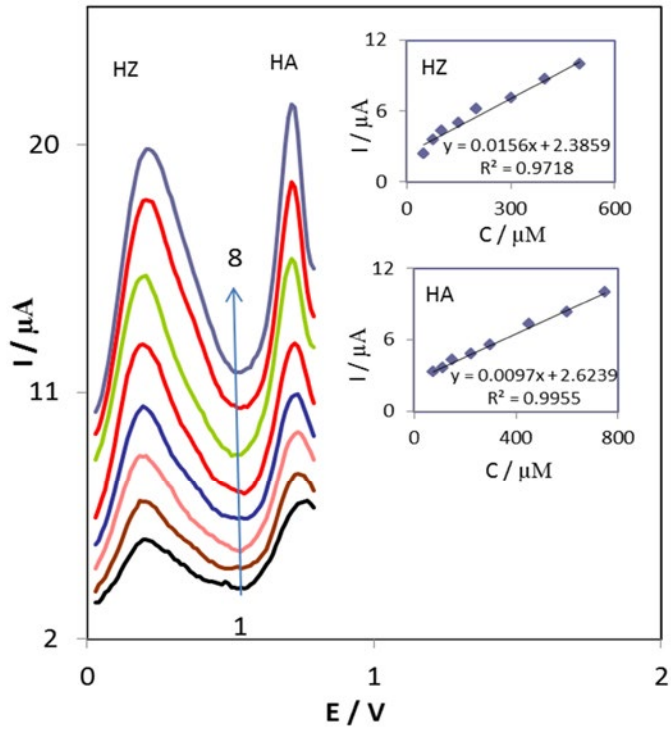

Fig. 7. DPVs of Fe_3O_4 / GCE in 0.1 M PBS (pH 8.0) containing different concentrations of HZ + HA in µM, from inner to outer: 50.0 + 75.0, 100.0+ 150.0 + 200.0+ 300.0 + 400.0 + 500.0, and 75.0 + 112.5 + 150.0+ 225.0 + 300.0 + 450.0+ 600.0+ 750.0, respectively.

ACKNOWLEDGMENTS

The authors wish to thank the Yazd University Research Council and Excellence in Sensors for financial support of this research.

CONFLICT OF INTEREST

The authors declare that there is no conflict of interests regarding the publication of this manuscript.

REFERENCES

1. Liu N, Xu YD, Li H, Li GH, Zhang LD. Effect of nano-micro TiN addition on the microstructure and mechanical properties of TiC based cermets. Journal of the European Ceramic Society. 2002;22(13):2409-14.
2. Mazloum-Ardakani M, Khoshroo A. High sensitive sensor based on functionalized carbon nanotube/ionic liquid nanocomposite for simultaneous determination of norepinephrine and serotonin. Journal of Electroanalytical Chemistry. 2014;717-718:17-23.
3. Mazloum-Ardakani M, Sabaghian F, Khoshroo A, Naeimi H. Simultaneous determination of the concentrations of isoproterenol, uric acid, and folic acid in solution using a novel nanostructure- based electrochemical sensor. Chinese Journal of Catalysis. 2014;35(4):565-72.
4. Kargan NH, Aliahmad M, Azizi S. Detecting Ultra-Violet Radiation by Using Titanium Dioxide Nanoparticles. Soft Nanoscience Letters. 2012;02(03):29-33.
5. He Z, Gao C, Qian M, Shi Y, Chen J, Song S. Electro-Fenton Process Catalyzed by Fe3O4 Magnetic Nanoparticles for Degradation of C.I. Reactive Blue 19 in Aqueous Solution: Operating Conditions, Influence, and Mechanism. Industrial & Engineering Chemistry Research. 2014;53(9):3435-47.
6. Tahir AA, Wijayantha KGU, Saremi-Yarahmadi S, Mazhar M, McKee V. Nanostructured Î±-Fe2O3Thin Films for Photoelectrochemical Hydrogen Generation. Chemistry of Materials. 2009;21(16):3763-72.
7. Jang JS, Lee J, Ye H, Fan F-RF, Bard AJ. Rapid Screening of Effective Dopants for Fe2O3 Photocatalysts with Scanning Electrochemical Microscopy and Investigation of Their Photoelectrochemical Properties. The Journal of Physical Chemistry C. 2009;113(16):6719-24.
8. Berry CC, Curtis ASG. Functionalisation of magnetic nanoparticles for applications in biomedicine. Journal of Physics D: Applied Physics. 2003;36(13):R198-R206.
9. Serov A, Kwak C. Direct hydrazine fuel cells: A review. Applied Catalysis B: Environmental. 2010;98(1-2):1-9.
10. ad. Ind Eng Chem. 1966;58(9):10.
11. Weisberg A. EXTRARENAL HYPERNEPHROMA. AMA Archives of Internal Medicine. 1954;94(2):314.
12. Devasenathipathy R, Palanisamy S, Chen S-M, Karuppiah C, Mani V, Ramaraj SK, et al. An Amperometric Biological Toxic Hydrazine Sensor Based on Multiwalled Carbon Nanotubes and Iron Tetrasulfonated Phthalocyanine Composite Modified Electrode. Electroanalysis. 2015;27(6):1403-10.
13. Mohammadi SZ, Beitollahi H, Bani Asadi E. Electrochemical determination of hydrazine using a ZrO2 nanoparticles-modified carbon paste electrode. Environmental Monitoring and Assessment. 2015;187(3).

14. Mazloum-Ardakani M, Khoshroo A, Hosseinzadeh L. Application of graphene to modified ionic liquid graphite composite and its enhanced electrochemical catalysis properties for levodopa oxidation. Sensors and Actuators B: Chemical. 2014;204:282-8.
15. Mazloum-Ardakani M, Hosseinzadeh L, Khoshroo A, Naeimi H, Moradian M. Simultaneous Determination of Isoproterenol, Acetaminophen and Folic Acid Using a Novel Nanostructure-Based Electrochemical Sensor. Electroanalysis. 2013;26(2):275-84.
16. Shamsipur M, Karimi Z, Tabrizi MA, Shamsipur A. Electrocatalytic Determination of Traces of Hydrazine by a Glassy Carbon Electrode Modified with Palladium-Gold Nanoparticles. Electroanalysis. 2014;26(9):1994-2001.
17. Mazloum-Ardakani M, Khoshroo A. An electrochemical study of benzofuran derivative in modified electrode-based CNT/ionic liquids for determining nanomolar concentrations of hydrazine. Electrochimica Acta. 2013;103:77-84.
18. Mahmoudi Moghaddam H, Beitollahi H, Tajik S, Sheikhshoaie I, Biparva P. Fabrication of novel TiO2 nanoparticles/Mn(III) salen doped carbon paste electrode: application as electrochemical sensor for the determination of hydrazine in the presence of phenol. Environmental Monitoring and Assessment. 2015;187(7).
19. Hosseini M, Momeni MM. Silver nanoparticles dispersed in polyaniline matrixes coated on titanium substrate as a novel electrode for electro-oxidation of hydrazine. Journal of Materials Science. 2010;45(12):3304-10.
20. Devasenathipathy R, Mani V, Chen S-M, Arulraj D, Vasantha VS. Highly stable and sensitive amperometric sensor for the determination of trace level hydrazine at cross linked pectin stabilized gold nanoparticles decorated graphene nanosheets. Electrochimica Acta. 2014;135:260-9.
21. Rosca V, Koper MTM. Electrocatalytic oxidation of hydrazine on platinum electrodes in alkaline solutions. Electrochimica Acta. 2008;53(16):5199-205.
22. Pinter JS, Brown KL, DeYoung PA, Peaslee GF. Amperometric detection of hydrazine by cyclic voltammetry and flow injection analysis using ruthenium modified glassy carbon electrodes. Talanta. 2007;71(3):1219-25.
23. Tauszik GR, Crocetta P. Production of hydroxylamine from nitrogen oxide: A short review. Applied Catalysis. 1985;17(1):1-21.
24. Coleman MD. Dapsone: modes of action, toxicity and possible strategies for increasing patient tolerance. British Journal of Dermatology. 1993;129(5):507-13.
25. Mazloum-Ardakani M, Khoshroo A, Hosseinzadeh L. Simultaneous determination of hydrazine and hydroxylamine based on fullerene-functionalized carbon nanotubes/ionic liquid nanocomposite. Sensors and Actuators B: Chemical. 2015;214:132-7.
26. Laurent S, Forge D, Port M, Roch A, Robic C, Vander Elst L, et al. ChemInform Abstract: Magnetic Iron Oxide Nanoparticles: Synthesis, Stabilization, Vectorization, Physicochemical Characterizations, and Biological Applications. ChemInform. 2008;39(35).
27. Sun Y-k, Ma M, Zhang Y, Gu N. Synthesis of nanometer-size maghemite particles from magnetite. Colloids and Surfaces A: Physicochemical and Engineering Aspects. 2004;245(1-3):15-9.
28. Jolivet J-P, Chanéac C, Tronc E. Iron oxide chemistry. From molecular clusters to extended solid networks. Chem Commun. 2004(5):477-83.
29. Suresh R, Giribabu K, Manigandan R, Vijayalakshmi L, Stephen A, Narayanan V. Electrocatalytic Property of Nano-Fe_3O_4 Modified Glassy Carbon Electrode. Advanced Materials Research. 2012;584:272-5.